Stromal Transforming Growth Factor-β Signaling Mediates Prostatic Response to Androgen Ablation by Paracrine Wnt Activity

Veronica R. Placencio,[1] Ali-Reza Sharif-Afshar,[2] Xiaohong Li,[2] Hongxia Huang,[2] Consolate Uwamariya,[2] Eric G. Neilson,[3] Michael M. Shen,[4] Robert J. Matusik,[1,2] Simon W. Hayward,[1,2] and Neil A. Bhowmick[1,2]

Departments of [1]Cancer Biology, [2]Urologic Surgery, and [3]Medicine, Vanderbilt-Ingram Cancer Center, Vanderbilt University, Nashville, Tennessee and [4]Department of Medicine and Genetics and Development, Columbia University Medical Center, New York, New York

Abstract

Mechanisms of androgen dependence of the prostate are critical to understanding prostate cancer progression to androgen independence associated with disease mortality. Transient elevation of transforming growth factor-β (TGF-β) occurs after androgen ablation. To determine the role of TGF-β on prostate response to androgen ablation, conditional TGF-β type II receptor knockout mouse models of the epithelia ($Tgfbr2^{NKX3.1KO}$) and stromal fibroblasts ($Tgfbr2^{fspKO}$) were used. After castration, the prostates of $Tgfbr2^{NKX3.1KO}$ mice had apoptosis levels similar to those expected for control $Tgfbr2^{floxE2/floxE2}$ mice. Prostates of $Tgfbr2^{fspKO}$ mice, however, had reduced regression and high levels of proliferation associated with canonical Wnt activity throughout the glandular epithelia regardless of androgen status. In contrast, $Tgfbr2^{floxE2/floxE2}$ prostates had epithelial canonical Wnt activity only in the surviving proximal ducts after castration. *In vitro* studies showed that androgen antagonist, bicalutamide, transiently elevated both $Tgfbr2^{floxE2/floxE2}$ and $Tgfbr2^{fspKO}$ stromal expression of Wnt-2, Wnt-3a, and Wnt-5a. The neutralization of Wnt signaling by the expression of secreted frizzled related protein-2 (SFRP-2) resulted in decreased LNCaP prostate epithelial cell proliferation in stromal conditioned media transfer experiments. *In vivo* tissue recombination studies using $Tgfbr2^{fspKO}$ prostatic stromal cells in combination with wild-type or SV40 large T antigen expressing epithelia resulted in prostates that were refractile to androgen ablation. The expression of SFRP-2 restored the $Tgfbr2^{fspKO}$-associated prostate responsiveness to androgen ablation. These studies reveal a novel TGF-β, androgen, and Wnt paracrine signaling axis that enables prostatic regression of the distal ducts after androgen ablation while supporting proximal duct survival. [Cancer Res 2008;68(12):4709–18]

Introduction

Prostate cancer continues to be a major cause of death in aging men (1). The prostate is an androgen-dependent organ. As a result, treatment for prostate cancer includes the inhibition of androgens. Regardless of the initial positive response to androgen ablation, the cancer frequently overcomes its dependence on androgens and results in a drug-resistant cancer with few options for treatment. Although androgen ablation therapy is intended to target the prostate epithelia, the influence of the prostatic stroma on androgen responsiveness of the adjacent epithelia is likely to be critical in the long-term effectiveness of treatment.

Mature and differentiated prostate tissue is formed and maintained by effects on androgen receptors within the stromal compartment (2, 3). The concept of mesenchymal cells relaying androgen sensitivity to the epithelia through paracrine interactions is supported by tissue recombination experiments. Prostate epithelia expressing a nonfunctional androgen receptor were equally sensitive to androgen ablation, carried out by castration of host mice, when compared with the control tissue recombinations generated with wild-type mesenchyme and wild-type epithelia (4, 5). Yet mesenchymal cells with a nonfunctional androgen receptor did not even support prostate epithelial development (6). This suggested that the prostatic stroma plays an instructive role in glandular development and potentially influences responsiveness to androgen ablation in prostate cancer progression (5). As a basis to understanding androgen-independent prostate cancer, we investigated the mechanism for prostate epithelial survival in the absence of androgens.

After androgen ablation, the prostate undergoes apoptotic regression. In mouse models, reintroduction of androgens after androgen ablation results in prostate regrowth originating from the proximal ducts. This observation indicates that the proximal ducts are inherently refractory to androgen ablation (7–9). Canonical Wnt signaling is known to play a role in cell survival in many tissues (10–12). Thus, we wanted to investigate a potential role for Wnt signaling in the survival of proximal ductal tissue upon castration. Another growth factor, transforming growth factor-β (TGF-β), is thought to support prostatic apoptosis as its expression coincides with androgen ablation in benign and cancer tissues (13–15). TGF-β binds the TGF-β type II receptor (Tgfbr2) at the cell surface to phosphorylate the TGF-β type I receptor and activate cytoplasmic proteins, predominantly Smad2 and Smad3 (16). Both cooperative and antagonistic interactions of Wnt, androgen, and TGF-β signaling pathways occur in the prostatic epithelia (17–20). However, the role of Wnt and TGF-β signaling on androgen dependence of the prostate is unknown.

We tested the hypothesis that paracrine Wnt signaling regulates stromal-epithelial interactions in response to androgen ablation in a TGF-β–dependent manner using mouse and allografting models. Canonical Wnt signaling involves the activation of cognate frizzled receptors at the cell surface that mediate β-catenin accumulation leading to transcriptional activity in the nucleus (21). Here, we report that canonical Wnt activity is present in the prostatic epithelia of the proximal ducts of the prostate after androgen

Note: Supplementary data for this article are available at Cancer Research Online (http://cancerres.aacrjournals.org/).

Requests for reprints: Neil A. Bhowmick, Department of Urologic Surgery, A-1302 Medical Center North, 1161 21st Avenue South, Nashville, TN 37232. Phone: 615-343-7140; Fax: 615-322-5869; E-mail: neil.bhowmick@vanderbilt.edu.

doi:10.1158/0008-5472.CAN-07-6289

ablation. Previously, we generated a Tgfbr2 conditional fibroblast knockout mouse through FSP-1 Cre-mediated recombination of Tgfbr2 exon 2 ($Tgfbr2^{fspKO}$), which resulted in the development of preneoplastic lesions (prostatic intraepithelial neoplasia) by 5 to 7 weeks of age (22). To further study the role of TGF-β on the prostate epithelia after androgen ablation, here, we developed a conditional epithelial Tgfbr2 knockout by crossing NKX3.1-Cre mice with $Tgfbr2^{floxE2/floxE2}$ mice (23), termed $Tgfbr2^{NKX3.1KO}$. Another valuable tool was the Tg(Fos-lacZ)34Efu/J mouse model, termed TOPGal, which enabled the visualization of canonical Wnt signaling activity (24). Interestingly, the prostates of $Tgfbr2^{fspKO}$ mice had constitutive Wnt signaling throughout the prostate and were resistant to androgen ablation–induced regression. The 12T7f LADY mouse model served as a transformed epithelial counterpart, expressing SV40 large T antigen in the prostatic epithelia (25). Tissue recombination allografting of the $Tgfbr2^{fspKO}$ prostatic stroma was able to convert the androgen-dependent 12T7f LADY prostatic epithelia to become refractile to androgen ablation. Together, the data provide a mechanism for androgen-independent survival of the prostate epithelia.

Materials and Methods

Transgenic mice. $Tgfbr2^{floxE2/floxE2}$ (23) and $Tgfbr2^{fspKO}$ mice of C57BL/6 background were generated as previously described (22). The NKX3.1-Cre mice, also in the C57BL/6 background, were crossed with $Tgfbr2^{floxE2/floxE2}$ mice to generate the $Tgfbr2^{NKX3.1KO}$ mouse model. The $Tgfbr2^{NKX3.1KO}$ mice were further crossed with Rosa26 mice to enable visualization of cells undergoing Cre-mediated recombination. TOPGal mice (24) were purchased from The Jackson Laboratory and crossed with $Tgfbr2^{floxE2/floxE2}$ and $Tgfbr2^{floxE2/wt}$-Cre^{FSP} mice to generate the $Tgfbr2^{floxE2/floxE2}$/TOPGal and $Tgfbr2^{fspKO}$/TOPGal mouse models. Prostatic epithelial organoids were generated from 15-wk-old 12T7f LADY mice, at which time they developed high-grade hyperplastic lesions and foci of adenocarcinoma (25, 26). All mice were genotyped from ear punch biopsies. NKX3.1-Cre mice were genotyped using the same Cre primers as the $Tgfbr2^{fspKO}$ mice (22). A single ~200-bp band indicated Cre expression. All other mouse genotyping was performed as previously reported (23–25). Harlan Sprague-Dawley SCID CB17/ICR hsd and C57BL/6 mice were used for tissue recombination and tissue rescue allografting techniques, respectively. All animal procedures were approved by the Vanderbilt Institutional Animal Care and Use Committee.

Cell culture. $Tgfbr2^{floxE2/floxE2}$ and $Tgfbr2^{fspKO}$ mouse primary prostate stromal cell cultures were generated from prostates of 6-wk-old to 8-wk-old mice, as described previously (27). Cultures grown between passages 10 and 30 were used for experiments. LNCaP cells were purchased and grown as recommended by American Type Culture Collection.

Conditioned media experiments and [^{3}H]thymidine incorporation. Conditioned stromal media was generated by plating 750,000 $Tgfbr2^{floxE2/floxE2}$ or $Tgfbr2^{fspKO}$ cells or for control 3,000,000 LNCaP cells on a 100-mm dish similar to previously published reports (28). $Tgfbr2^{floxE2/floxE2}$ and $Tgfbr2^{fspKO}$ stromal cells were transduced with either green fluorescent protein (GFP; control) or secreted frizzled related protein-2 (SFRP-2) adenovirus at 10^5 virus particles/mL for 24 h before replacing standard stromal cell culture media with 5% serum containing media to allow virus production in stromal cells. The stromal cells were incubated for 72 h in the stromal cell media containing 10^{-8} mol/L testosterone or, if indicated, bicalutamide (10^{-5} mol/L). The stromal conditioned media was transferred to 15 mL conical tubes and stored in −80°C at least 24 h up to 3 wk. The stromal conditioned media was thawed and plated over LNCaP cells (10,000 per well) in 24-well plates. The conditioned media was replaced after 72 h of incubation with fresh conditioned media. In select conditions, fresh bicalutamide was also included as part of the conditioned media. After 120 h of incubation of LNCaP cells with stromal conditioned media, [^{3}H]thymidine incorporation assays were performed. Three hours before assaying for proliferation, cells were given 2 μCi [^{3}H]thymidine (PerkinElmer) in serum-free RPMI per well. Cells were washed in 1 mL 10% TCA for 10 min thrice then lysed with 300 μL 200 mmol/L NaOH for 30 min. The cell lysates (100 μL) were measured for [^{3}H]thymidine activity using a scintillation counter (29). All treatment conditions were performed in triplicate.

Immunohistochemistry. Tissues were fixed with 4% paraformaldehyde, embedded in paraffin, and sectioned for histologic analysis. GFP (1:1,000; Santa Cruz Biotechnology), Ki67 (1:3,000, Vector Laboratories), and SV40 (1:1,000,Calbiochem) immunohistochemistry was performed by using antigen retrieval with antigen unmasking solution (Vector Laboratories) diluted 1:100. After primary antibody incubation overnight, Dako Cytomation universal or rabbit kits were used for the secondary antibody and development with 3,3′-diaminobenzidine. Terminal uridine deoxynucleotidyl transferase dUTP nick end labeling (TUNEL) staining was performed using the ApopTag Peroxidase *In situ* Apoptosis Detection kit (Chemicon). Double immunohistochemical staining was performed for TUNEL followed by staining for β-galactosidase (1:5,000; Abcam) developed with TrueBlue Peroxidase Substrate (KPL). Immunohistochemical staining was systematically quantitated by taking a ratio of positively stained cells per epithelial nuclei per field (200×). Statistical significance was determined by two-tailed Student's *t* test.

Immunofluorescence. Cells (50,000) were treated with 5 ng/mL TGF-β (Cell Sciences) on glass coverslips for 16 h. The cells were fixed with 4% paraformaldehyde for 10 min at 4°C. Smad2 localization was visualized using primary (1:1,000; Santa Cruz Biotechnology) and secondary antigoat Alexa Fluor 594 antibody (1:500; Invitrogen) on a Nikon epifluorescence microscope.

β-Galactosidase tissue staining. Whole mouse prostates were dissected and fixed in 4% PFA for 1 to 2 h, washed in PBS, incubated with X-gal for 3 h at 30°C, washed in PBS, and fixed in 4% PFA overnight. Processed paraffin-embedded tissues were sectioned at 8 μm and counterstained with Nuclear Fast Red (Electron Microscopy Sciences).

Tissue recombination allografting. The tissue recombinations were performed as previously described (30). Epithelial organoids were derived by digesting prostates of 6-wk-old to 12-wk-old wild-type C57BL/6 mice or 15-wk-old LADY 12T7f mice in 675 units/mL collagenase with 0.04% DNase type I at 37°C for 40 min as previously described (30). The organoids were washed and pipetted into 50 μL collagen with stromal cells from $Tgfbr2^{floxE2/floxE2}$ or $Tgfbr2^{fspKO}$ mouse prostates and allowed to incubate overnight at 37°C. The tissue recombinants were then allografted under the renal capsule of syngenic C57BL/6 for 5 to 7 wk or SCID mice for 6 wk. Castration of host mice was performed 3 to 7 d before sacrifice as indicated.

RNA purification and reverse transcription–PCR. RNA from cell lysates was purified using the RNeasy mini kit (Qiagen) according to the manufacturer's directions. Reverse transcription–PCR (RT-PCR) was performed for 32 cycles with the following primer sets: Wnt-2 forward 5′GTTTGCCCGTGCCTTTGTAGATG and reverse 5′CCGGGTGACGTGGATGTG, Wnt-3a forward 5′TCTGCAGGAACTACGTGGAGATCA and reverse 5′TCCCGAGAGACCATTCCTCCAAAT, Wnt-5a forward 5′TCGCCATGAAGAAGCCCATTGGAA and reverse 5′TGTCCTTGAGAAAGTCCTGCCAGT, Wnt-9a forward 5′ACTGCTTTCCTCTACGCCATCTCT and reverse 5′TTTGCAAGTGGTTTCCACTCCAGC, Wnt-11 forward 5′CTGACATGCGCTGGAACTGCTC and reverse 5′AGGCCCGGGCGATGGTGT, and 18S forward 5′ CAAGAACGAAAGTCGGAGGTTC and reverse 5′ GGACATCTAAGGGCATCACAG.

Results

Stromal TGF-β responsiveness enables prostatic regression after androgen depletion. Androgen ablation causes prostate regression with a transient elevation of TGF-β expression (13). However, the role of TGF-β on the prostate after androgen ablation is not clear. We first developed a conditional Tgfbr2 knockout targeted to the epithelia by crossing NKX3.1-Cre mice with $Tgfbr2^{floxE2/floxE2}$ mice, termed $Tgfbr2^{NKX3.1KO}$ (conditional epithelial Tgfbr2 knockout). Further crossing the $Tgfbr2^{NKX3.1KO}$ mice

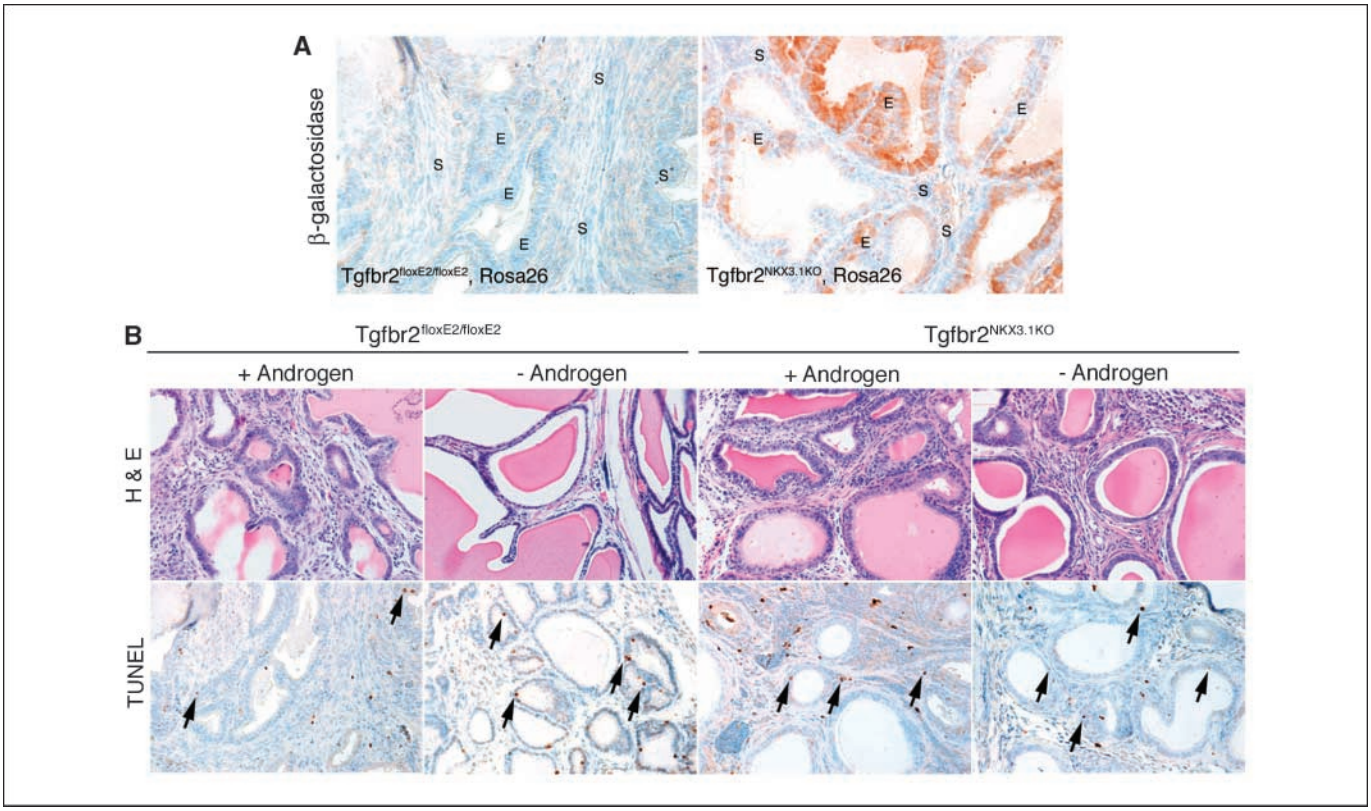

Figure 1. Conditional knockout of *Tgfbr2* in the prostate epithelia (Tgfbr2$^{NKX3.1KO}$) did not significantly affect the response to androgen ablation compared with control Tgfbr2$^{floxE2/floxE2}$ prostate allografts. *A,* immunohistochemistry for β-galactosidase expression (*brown*) in tissue rescued Tgfbr2$^{NKX3.1KO}$/Rosa26 prostates indicates Cre recombination in the prostatic epithelia compared with control Tgfbr2$^{floxE2/floxE2}$/Rosa26 prostates with no detectable staining. Sections were counterstained with hematoxylin (*blue*). The epithelial (*E*) and stromal (*S*) compartments are indicated. *B, top,* H&E staining of Tgfbr2$^{NKX3.1KO}$ and Tgfbr2$^{floxE2/floxE2}$ tissue rescue allografts suggests similar prostatic development (n = 4); *bottom,* TUNEL staining (*brown*) indicates differential apoptosis of the prostatic epithelia of Tgfbr2$^{NKX3.1KO}$ and Tgfbr2$^{floxE2/floxE2}$ allografts in hosts that were not castrated (+*Androgen*) compared with hosts that were castrated (−*Androgen*). Increased TUNEL-positive epithelia after castration indicates responsiveness to androgen ablation. The increase in TUNEL-positive epithelia in intact compared with castrated Tgfbr2$^{floxE2/floxE2}$ prostates was significant (P = 0.0379). The increase in TUNEL-positive epithelia in intact compared with castrated Tgfbr2$^{NKX3.1KO}$ prostates was significant (P = 0.0056). Student's t test evaluation determined P value of <0.05 is significant.

into the Rosa26 line enabled the immunohistochemical localization of β-galactosidase expression associated with Cre-mediated recombination in the prostatic epithelia (Fig. 1*A*). Because the Tgfbr2$^{NKX3.1KO}$ mice died perinatally, the prostates of these and Tgfbr2$^{floxE2/floxE2}$ mice were rescued to the renal capsule of syngenic C57BL/6 male hosts. H&E staining revealed little difference in the ductal structures of the Tgfbr2$^{NKX3.1KO}$ prostates compared with Tgfbr2$^{floxE2/floxE2}$ controls (Fig. 1*B*). However, the Tgfbr2$^{NKX3.1KO}$ prostates had significantly higher epithelial turnover as shown by the apoptotic TUNEL staining (Fig. 1*B, bottom*) compared with Tgfbr2$^{floxE2/floxE2}$ allografts. After castration, there was a further elevation of epithelial TUNEL staining in the Tgfbr2$^{NKX3.1KO}$ prostates as observed in Tgfbr2$^{floxE2/floxE2}$ allografts. Taken together, there was no significant difference in apoptotic response observed between Tgfbr2$^{floxE2/floxE2}$ and Tgfbr2$^{NKX3.1KO}$ prostates after castration compared with their intact controls, respectively.

As epithelial TGF-β signaling did not seem to affect androgen responsiveness, the role of stromal TGF-β signaling was studied using the Tgfbr2^{fspKO} mouse model (conditional stromal Tgfbr2 knockout). The castration of Tgfbr2$^{floxE2/floxE2}$ mice resulted in 42% and 55% decrease in the total prostate wet weights, after 7 and 14 days, respectively (Fig. 2*A*). In contrast, there was a negligible decrease in Tgfbr2^{fspKO} prostates wet weight 7 days after castration, with ~20% regression by 14 days. Histologic analysis revealed that, 7 days after castration, the Tgfbr2$^{floxE2/floxE2}$ prostates, with otherwise low cellular turnover, had an expected increase in TUNEL-positive apoptotic cells in both the epithelial and stromal compartments and little evidence of proliferation observed by Ki67 staining (Fig. 2*B*). Before castration, Tgfbr2^{fspKO} mice exhibited slightly higher rates of apoptosis than Tgfbr2$^{floxE2/floxE2}$ mice (1.4-fold), accompanied by significant proliferation consistent with the described PIN phenotype (22). Seven days after castration, prostates from Tgfbr2^{fspKO} mice had little apparent epithelial apoptosis, yet remained highly proliferative based on TUNEL and Ki67 staining, respectively. The apparent elevated proliferation of the Tgfbr2^{fspKO} stroma coincided with greater stromal expansion compared with Tgfbr2$^{floxE2/floxE2}$ prostates. Together, these data suggested that normal prostate epithelial regression occurs in response to stromal TGF-β signals.

Before further studying the androgen independence of the prostates in Tgfbr2^{fspKO} mice, we needed to establish that the epithelial response resulted from the prostatic stroma and not other systemic factors in these mice. The FSP-1 Cre promoter targets a subset of fibroblasts throughout the body, including prostatic fibroblasts (22, 31). We verified the loss of TGF-β responsiveness in Tgfbr2^{fspKO} cultured stromal cells by immunolocalization of Smad2 (Fig. 3*A*). A tissue recombination allograft

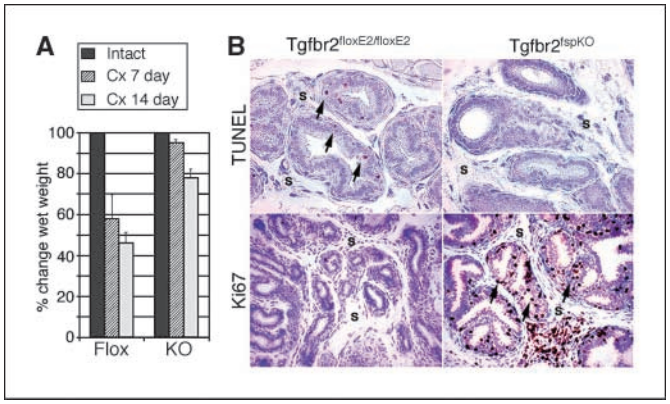

Figure 2. Tgfbr2^{fspKO} prostates lose androgen responsiveness after androgen ablation. *A*, percentage change in total wet prostate weight is shown 7 and 14 d after castration (*Cx*). Average Tgfbr2$^{floxE2/floxE2}$ and Tgfbr2^{fspKO} total wet prostate weights are shown as a percentage of the respective total prostate weight from intact Tgfbr2$^{floxE2/floxE2}$ (*Flox*) and Tgfbr2^{fspKO} (*KO*) mice (n = 5). *B*, 3 d after castration, DL prostate lobes of Tgfbr2$^{floxE2/floxE2}$ and Tgfbr2^{fspKO} mice were subjected to TUNEL staining (*brown*), indicating apoptotic cells and Ki67 staining (*brown*) indicating proliferative cells. Hematoxylin (*blue*) was used as a nuclear counter stain. The stromal (*S*) compartment is indicated and black arrows indicate positively stained epithelial cells. Prostates were dissected from 5-wk-old to 7-wk-old male mice. Dorsolateral lobes are shown and these effects are consistent with all other lobes (n = 8). The increase in TUNEL positive Tgfbr2^{fspKO} epithelia after castration was significantly greater than Tgfbr2$^{floxE2/floxE2}$ epithelia (P value = 0.0152). The level of Ki67 positive Tgfbr2^{fspKO} epithelia after castration was significantly greater than Tgfbr2$^{floxE2/floxE2}$ epithelia (P = 0.0003).

approach was then used to identify the role of the prostatic stromal cells in the phenotype observed. The tissue recombination technique consisted of combining cultured stromal cells derived from Tgfbr2$^{floxE2/floxE2}$ or Tgfbr2^{fspKO} prostates with epithelial organoids isolated by digesting mature wild-type C57BL/6 mouse prostates. The tissue recombinants were allografted to the subrenal capsules of syngeneic male mice (32). Five weeks after grafting, the Tgfbr2$^{floxE2/floxE2}$ and Tgfbr2^{fspKO} stromal cells organized themselves around the epithelial organoids to form prostatic glands (Fig. 3*B*). Seven days after castration of the hosts, there was a 6-fold increase in TUNEL-positive epithelia in the Tgfbr2$^{floxE2/floxE2}$ stroma-associated glands (Fig. 3*C*). Note, in comparison, the Tgfbr2^{fspKO} stroma-associated glands did not show a significant increase in TUNEL-positive epithelia. Ki67 staining indicated minimal proliferation in recombinants associated with Tgfbr2$^{floxE2/floxE2}$ stroma after castration (Fig. 3*D*). In contrast, the recombinants associated with Tgfbr2^{fspKO} stroma had greater epithelial proliferation after castration. Collectively, castration of the host mice resulted in regression of the allografted tissue recombinants associated with Tgfbr2$^{floxE2/floxE2}$, but not Tgfbr2^{fspKO} stromal cells. These observations further supported that the androgen ablation refractile phenotype of our Tgfbr2^{fspKO} mice resulted from interactions within the prostate microenvironment.

Proximal ductal epithelial activation of Wnt signaling after androgen ablation mediates stromal-epithelial crosstalk. The next step was to determine how TGF-β signaling within the stroma was responsible for the observed regression in the Tgfbr2$^{floxE2/floxE2}$ or lack thereof in the Tgfbr2^{fspKO} mouse prostates. The proximal ducts of the prostate remain viable as the distal ducts regress in the absence of androgen signaling. Up-regulation of Wnt ligands and activating mutations of β-catenin in prostate cancer epithelium is a potential mechanism for androgen refractory prostatic epithelial proliferation (33–35). To address the potential of a Wnt signaling mechanism to support the androgen-independent prostate survival phenotype observed, we developed a Tgfbr2^{fspKO}/TOPGal mouse model (conditional stromal Tgfbr2 knockout with a canonical Wnt signaling reporter). Intact and castrated male Tgfbr2$^{floxE2/floxE2}$/TOPGal and Tgfbr2^{fspKO}/TOPGal prostates were subjected to whole mount β-galactosidase staining to visualize canonical Wnt activity. In whole mount staining of prostates from intact Tgfbr2$^{floxE2/floxE2}$/TOPGal mice, β-galactosidase expression was not detected (Fig. 4*A*). However, 3 days after castration, β-galactosidase activity was detected exclusively in the proximal ducts of the prostate indicating activated β-catenin signaling. This was further supported by elevated immunolocalization for β-galactosidase expression in the proximal glands of Tgfbr2$^{floxE2/floxE2}$/TOPGal prostates after castration (Supplementary Fig. S2). By the 7th day after castration, little β-galactosidase activity was detected in Tgfbr2$^{floxE2/floxE2}$/TOPGal prostates (data not shown). In contrast to that observed in Tgfbr2$^{floxE2/floxE2}$/TOPGal prostates, Fig. 4*A* showed that the Tgfbr2^{fspKO}/TOPGal prostates had β-galactosidase expression in the entire gland before castration with further elevated expression after castration. In both Tgfbr2$^{floxE2/floxE2}$/TOPGal and Tgfbr2^{fspKO}/TOPGal prostates, only the epithelial compartment showed strong positive β-galactosidase activity (Fig. 4*B* and *C*). Costaining for TUNEL and β-galactosidase in Tgfbr2$^{floxE2/floxE2}$/TOPGal flox prostate glands, 4 days after castration, illustrated that the epithelia expressing β-galactosidase did not overlap with epithelia undergoing apoptosis (Fig. 4*D*). This finding suggested that the epithelia in the proximal glands supported canonical Wnt activity during normal prostatic regression after androgen ablation. In addition, the hormone refractory Tgfbr2^{fspKO} prostates supported constitutive paracrine canonical Wnt signaling. The coincident localization of canonical Wnt signaling in Tgfbr2$^{floxE2/floxE2}$/TOPGal prostates and the reported region surviving androgen ablation supported the possibility of a causal relationship between the two events.

To determine if the observed epithelial Wnt activity could be due to stromal regulation of Wnt ligand production, Tgfbr2$^{floxE2/floxE2}$ and Tgfbr2^{fspKO} cultured prostatic stromal cells were treated with an androgen receptor antagonist, bicalutamide. The expression of Wnt ligands was measured after androgen ablation over a time course of 5 days by semiquantitative RT-PCR. There was a transient increase in Wnt-2, Wnt-3a, and Wnt-5a 1 and 3 days after bicalutamide treatment of Tgfbr2$^{floxE2/floxE2}$ stromal cells, with a decrease in expression by 5 days (Fig. 5*A*). A similar trend was seen with Tgfbr2^{fspKO} stromal cells, but with elevated basal expression for Wnt-2, Wnt-3a, and Wnt-5a. Wnt-9a and Wnt-11 expression were unchanged in both stromal cell types under the same conditions. When Tgfbr2$^{floxE2/floxE2}$ stromal cells were treated with bicalutamide and TGF-β, there was a lack of Wnt expression compared with treatment with bicalutamide alone (data not shown). Thus, inhibiting either the androgen or the TGF-β signaling pathway could induce Wnt-2, Wnt-3a, and Wnt-5a gene expression in prostatic stromal cells.

To determine the role of paracrine Wnt signaling on the epithelial response to androgen ablation, the proliferation of prostatic epithelial cells was measured in the presence of conditioned media collected from either Tgfbr2$^{floxE2/floxE2}$ or Tgfbr2^{fspKO} stromal cell cultures. As seen in Fig. 5*B*, bicalutamide

treatment had little proliferative effect on either stromal cell type grown in culture, as measured by [^{3}H]thymidine incorporation assays. As anticipated, the Tgfbr2^{fspKO} stromal cells were notably more proliferative than the Tgfbr2$^{floxE2/floxE2}$ stromal cells. Bicalutamide treatment decreased the proliferation of the androgen-responsive prostate cancer line, LNCaP epithelial cells, as expected. Therefore, LNCaP cells were subsequently used as the target epithelia to assess proliferative responsiveness to conditioned stromal media treatment and androgen ablation. Control GFP-transduced Tgfbr2$^{floxE2/floxE2}$-conditioned media had lower proliferative response on LNCaP cells compared with the enhanced proliferation using the GFP-transduced Tgfbr2^{fspKO}-conditioned media (Fig. 5*C*). Wnt expression by the stroma was antagonized through adenoviral expression of SFRP-2 to stromal cell cultures. The SFRP-2 transduced Tgfbr2^{fspKO}-conditioned media significantly decreased proliferation of LNCaP cells compared with GFP-transduced Tgfbr2^{fspKO}-conditioned media. Bicalutamide treatment to the Tgfbr2^{fspKO} stroma during generation of conditioned media (Bic on Stro) further decreased LNCaP proliferation, demonstrating the paracrine effect of androgen ablation on epithelial cells. However, most dramatic was the direct effect of androgen ablation on the epithelia with SFRP-2 transduced Tgfbr2^{fspKO}-conditioned stromal media (Bic on Epi), which resulted in a 50% decrease in LNCaP proliferation compared with the GFP-transduced Tgfbr2^{fspKO}-conditioned stromal media control. This suggested that Wnt ligands expressed by both Tgfbr2$^{floxE2/floxE2}$ and Tgfbr2^{fspKO} stromal cells support epithelial survival in response to androgen antagonism.

Next, the role of TGF-β on Wnt expression during androgen ablation in mice was determined. Previously, SFRP-2 has been shown to inhibit Wnt-3a and Wnt-5a *in vivo* (36, 37). Based on SFRP-2–mediated inhibition of prostatic epithelial cell proliferation *in vitro*, we hypothesized that it may restore androgen dependence to the Tgfbr2^{fspKO} prostate. The fragile condition of Tgfbr2^{fspKO} mice did not allow expression of SFRP-2 in these mice directly. Therefore, we transduced control GFP or SFRP-2 adenovirus in intact Tgfbr2$^{floxE2/floxE2}$ and Tgfbr2^{fspKO} prostate lobes and subsequently allografted the tissues under the renal capsules of SCID mice in tissue rescue experiments. GFP staining confirmed successful transduction of the allografted tissues (Supplementary Fig. S6). Three days after allografting, the host mice were either left intact or castrated for an additional 3 days. There were no observable differences in apoptotic rate resulting from the expression of GFP or SFRP-2 on Tgfbr2$^{floxE2/floxE2}$ and Tgfbr2^{fspKO} rescued prostates in the intact host mice based on TUNEL staining (Supplementary Fig. S4). After castration of the host mice, the Tgfbr2$^{floxE2/floxE2}$ prostates had the expected elevation of TUNEL staining in both GFP and SFRP-2 transduced prostates (Fig. 6*A* and *B*). The expression of GFP with Tgfbr2^{fspKO} prostates recapitulated the original observation of refractivity to androgen ablation. TUNEL-positive epithelia in GFP-Tgfbr2$^{floxE2/floxE2}$ prostates, 3 days after castration, were significantly elevated compared with GFP-Tgfbr2^{fspKO} prostates. Note, in comparison, the expression of SFRP-2 resulted in a 3-fold increase in the apoptosis of Tgfbr2^{fspKO} prostates after castration similar to Tgfbr2$^{floxE2/floxE2}$ prostates. The restoration of prostate regression in SFRP-2–Tgfbr2^{fspKO} prostates after castration indicated cooperation among the TGF-β, Wnt, and androgen signaling pathways.

Stromal TGF-β signaling allows prostatic ductal regression after androgen ablation in prostate cancer. Next, the role of

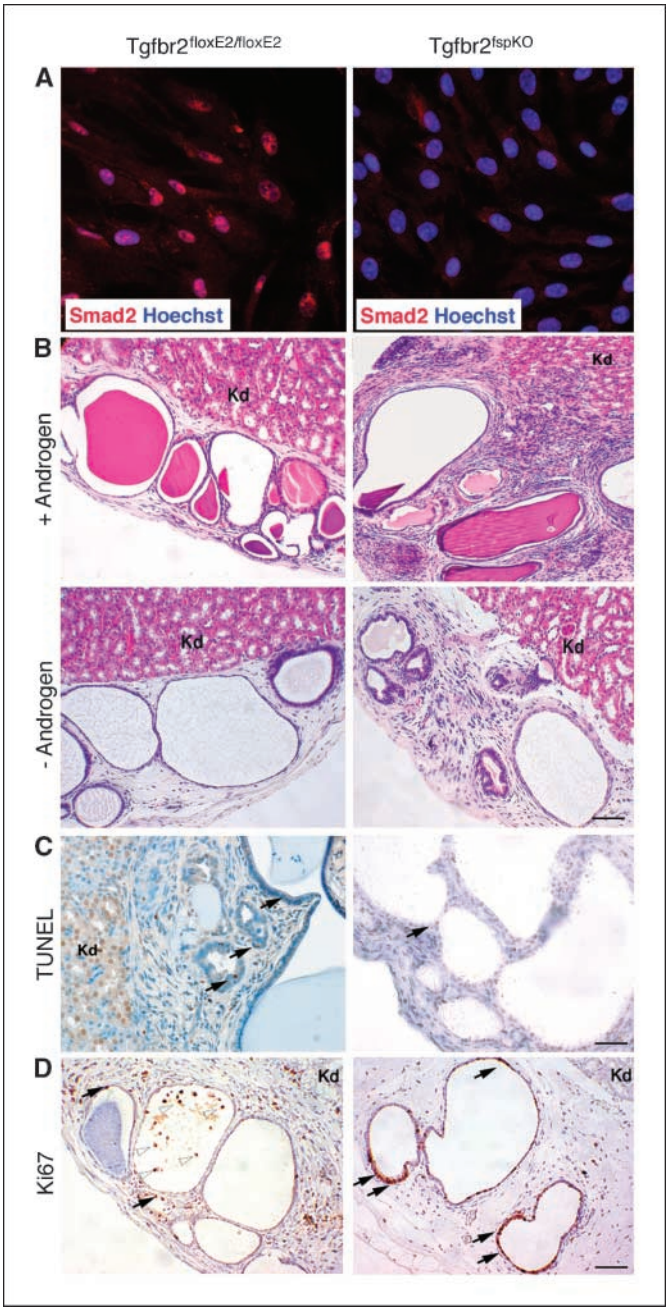

Figure 3. Loss of TGF-β responsiveness in prostatic stromal cells causes the prostate to become refractory to androgen ablation. *A,* to assess the competency of Tgfbr2$^{floxE2/floxE2}$ and Tgfbr2^{fspKO} prostatic stromal cells for TGF-β signaling, Smad2 was localized by Alexa Fluor 594 (*red*) immunofluorescence staining after TGF-β treatment. Hoechst nuclear counter stain was used (*blue*). Colocalization of Smad2 with Hoechst indicates active TGF-β signaling, whereas disparate staining indicates a lack of TGF-β signaling. *B,* H&E staining of prostatic glandular structures in tissue recombination grafts of Tgfbr2$^{floxE2/floxE2}$ and Tgfbr2^{fspKO} stromal cells with epithelial organoids were allografted for 6 wk in intact (*two top panels*) syngenic host male mice (+*Androgen*; $n = 8$) or castrated (*two bottom panels*) for the last week of grafting in syngenic host male mice (−*Androgen*; $n = 8$). *Kd,* kidney tissue. *Black bar,* 100 μm. *C,* TUNEL staining (*black arrows*) in Tgfbr2$^{floxE2/floxE2}$ and Tgfbr2^{fspKO} tissue recombination grafts from castrated mice ($n = 4$). The level of TUNEL positive Tgfbr2^{fspKO}-associated epithelia after castration was significantly lower than Tgfbr2$^{floxE2/floxE2}$-associated epithelia ($P = 0.0249$). *Black bar,* 50 μm. *D,* Ki67 staining (*black arrows*) indicate proliferative cells of Tgfbr2$^{floxE2/floxE2}$ and Tgfbr2^{fspKO} allografts from castrated mice ($n = 4$). *Open arrowheads,* background staining of likely dead cells. The level of Ki67 positive Tgfbr2^{fspKO}-associated epithelia after castration was significantly greater than Tgfbr2$^{floxE2/floxE2}$-associated epithelia ($P = 0.0030$). *Black bar,* 50 μm.

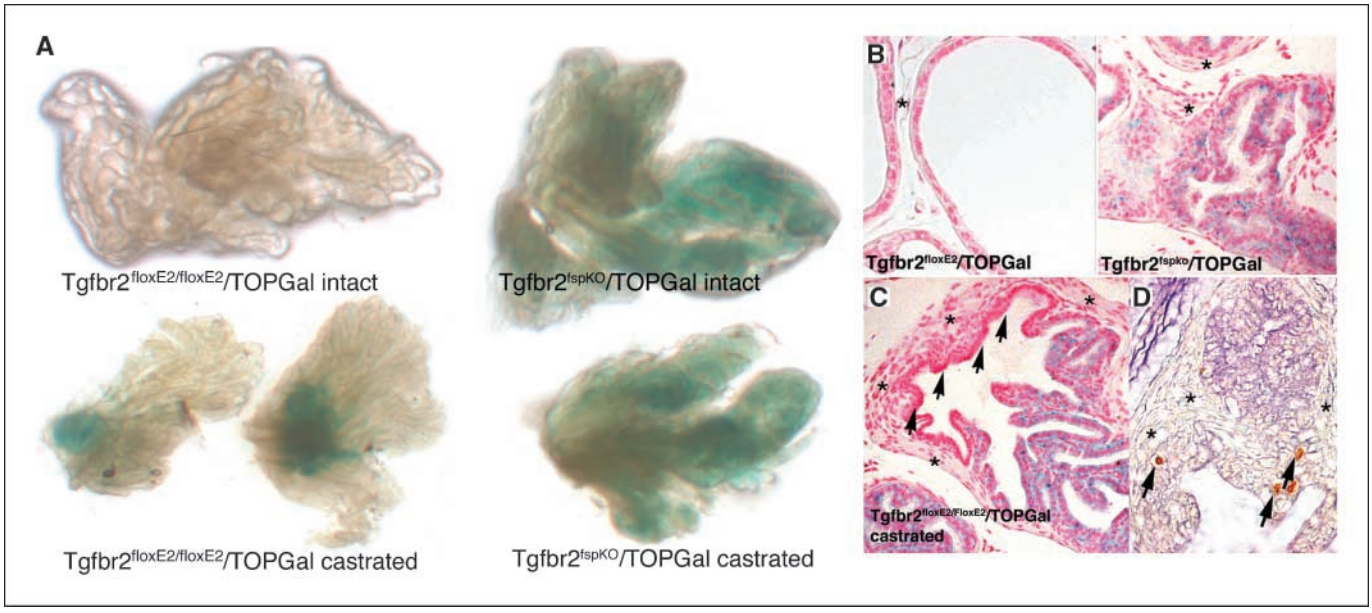

Figure 4. Inhibiting TGF-β signaling in the prostatic stroma results in constitutive Wnt signaling throughout the prostatic epithelia associated with survival after androgen ablation. Six-week-old TOPGal mice were stained for β-galactosidase activity and anterior and dorsolateral prostate lobes from intact and 3-d castrated mice were analyzed. *A,* Tgfbr2$^{floxE2/floxE2}$/TOPGal and Tgfbr2^{fspKO}/TOPGal prostates from intact and 3 d after castration were stained for β-galactosidase activity (*blue*) and imaged as whole mounts (n = 8) to show areas of canonical Wnt signaling activity. *B,* paraffin sections of the β-galactosidase–stained intact Tgfbr2$^{floxE2/floxE2}$/TOPGal and Tgfbr2^{fspKO}/TOPGal distal prostates were counterstained with Nuclear Fast Red. Asterisks indicate the stromal compartment. (Prostates from intact and castrated Tgfbr2^{fspKO}/TOPGal mice were similar. Only the intact Tgfbr2^{fspKO}/TOPGal tissue section is shown.) *C,* 3 d after castration, paraffin sections of the β-galactosidase–stained Tgfbr2$^{floxE2/floxE2}$/TOPGal prostate were counterstained with Nuclear Fast Red. Tissue section shows the distal prostate as it is regressing toward the proximal area. Asterisks indicate the stromal compartment. *D,* after castration of control Tgfbr2$^{floxE2/floxE2}$/TOPGal mice, the β-galactosidase activity–stained prostate sections were costained for TUNEL (*brown*) indicated with black arrows and β-galactosidase expression (*blue*; n = 4). Tissue section shows the distal prostate as it is regressing toward the proximal area. Asterisks indicate the stromal compartment, and black arrows indicate the epithelia with no β-galactosidase activity after castration (n = 8).

stromal TGF-β signaling in a prostate cancer model system was examined. Our objective was to determine if the paracrine instruction from the stroma to the epithelia observed in the development of androgen refractory PIN lesions continued to have an androgen refractory influence in the progression from PIN to adenocarcinoma. This was achieved by allografting tissue recombinants consisting of Tgfbr2$^{floxE2/floxE2}$ or Tgfbr2^{fspKO} stromal cells with prostate epithelial organoids from a prostate cancer mouse model expressing the SV40 large T antigen in the epithelia 12T7f LADY (25). Host male SCID mice were treated weekly with either SFRP-2 or GFP control adenovirus. Five weeks after allografting, half of the host mice were castrated. All grafts were analyzed 6 weeks after grafting. The GFP-Tgfbr2$^{floxE2/floxE2}$ stroma grafts (with LADY organoids) formed prostatic ductal structures with minimal hyperplasia (Supplementary Fig. S5*A* and *B*). After castration, the GFP-Tgfbr2$^{floxE2/floxE2}$ stroma-associated grafts had elevated TUNEL-positive apoptotic epithelia. In contrast, GFP-Tgfbr2^{fspKO} stroma-associated grafts developed adenocarcinoma (Fig. 6*C, top*). The GFP-Tgfbr2^{fspKO} stroma-associated grafts had low levels of apoptosis (Fig. 6*C, bottom*). SFRP-2–Tgfbr2$^{floxE2/floxE2}$ and GFP-Tgfbr2$^{floxE2/floxE2}$ stroma-associated grafts were similar with regard to apoptotic response to androgen ablation. Notably, the SFRP-2–Tgfbr2^{fspKO} stroma-associated grafts had elevated levels of TUNEL-positive epithelia after castration, typical of normal prostate regression (Fig. 6*D, bottom*). We also found that the SFRP-2–Tgfbr2^{fspKO} stroma-associated grafts seemed more differentiated than analogous GFP-Tgfbr2^{fspKO} stroma-associated grafts. Thus, stromal androgen and TGF-β signaling cooperates with epithelial Wnt signaling to regulate responsiveness to androgen ablation in benign, preneoplastic, and adenocarcinoma of the prostate.

Discussion

Our study showed that stromal responsiveness to TGF-β allows androgen sensitivity in the prostate epithelia through paracrine Wnt signaling. The direct role of TGF-β signaling on the prostate epithelia after castration was minimal based on histologic and apoptotic differences between the Tgfbr2$^{NKX3.1KO}$ and Tgfbr2$^{floxE2/floxE2}$ prostates. It is possible that compensatory signaling by activin and its cognate receptors may provide Smad protein activity similar to TGF-β. However, the conditional knockout of the TGF-β type II receptor in fibroblasts, in the Tgfbr2^{fspKO} mice and tissue recombinants, indicated the importance of TGF-β responsiveness in the stromal compartment after castration. Further crossing of the Tgfbr2^{fspKO} mice to the TOPGal reporter gene mouse model showed the regulatory role of stromal TGF-β signaling on Wnt signaling in epithelial cells refractory to androgen ablation. The Tgfbr2^{fspKO} stromal cells themselves acquired a more proliferative phenotype (presumably due to the loss of the growth inhibitory TGF-β signaling) and promoted nearby epithelia to increase their rate of proliferation and overcome hormonal dependence. The mechanisms behind the observed phenomena highlight a stromal derived paracrine Wnt signaling axis that is triggered upon androgen ablation. The stark proximal ductal localization of canonical Wnt signaling activity in control prostates after castration indicated duplicity of responses to androgen ablation, one of survival and another for cell death.

Thus, the data indicate that the role for TGF-β signaling after androgen ablation is to suppress Wnt signals in much of the distal prostate to enable regression.

Previous studies have shown that Wnt genes or proteins in the Wnt signaling pathway are up-regulated or mutated in androgen-independent prostate cancers (10, 11). Castration provided a transient elevation of canonical Wnt signaling in Tgfbr2$^{floxE2/floxE2}$ prostates (Fig. 4). In parallel, Tgfbr2$^{floxE2/floxE2}$ prostatic stromal cells transiently express specific Wnt genes in response to an androgen antagonist, bicalutamide (Fig. 5). In contrast, Tgfbr2^{fspKO} stromal cells had elevated basal expression of Wnt-2, Wnt-3a, and Wnt-5a. Recently, preosteoblasts were reported to induce Wnt signaling as a result of androgen stimulation, and through paracrine signaling, the preosteoblasts subsequently increased the proliferation of prostate cancer cells in a coculture system *in vitro* (38). As preosteoblasts and prostatic stromal cells are both of mesenchymal origin, together with the results presented, this suggests a directional regulation of paracrine Wnt signaling by

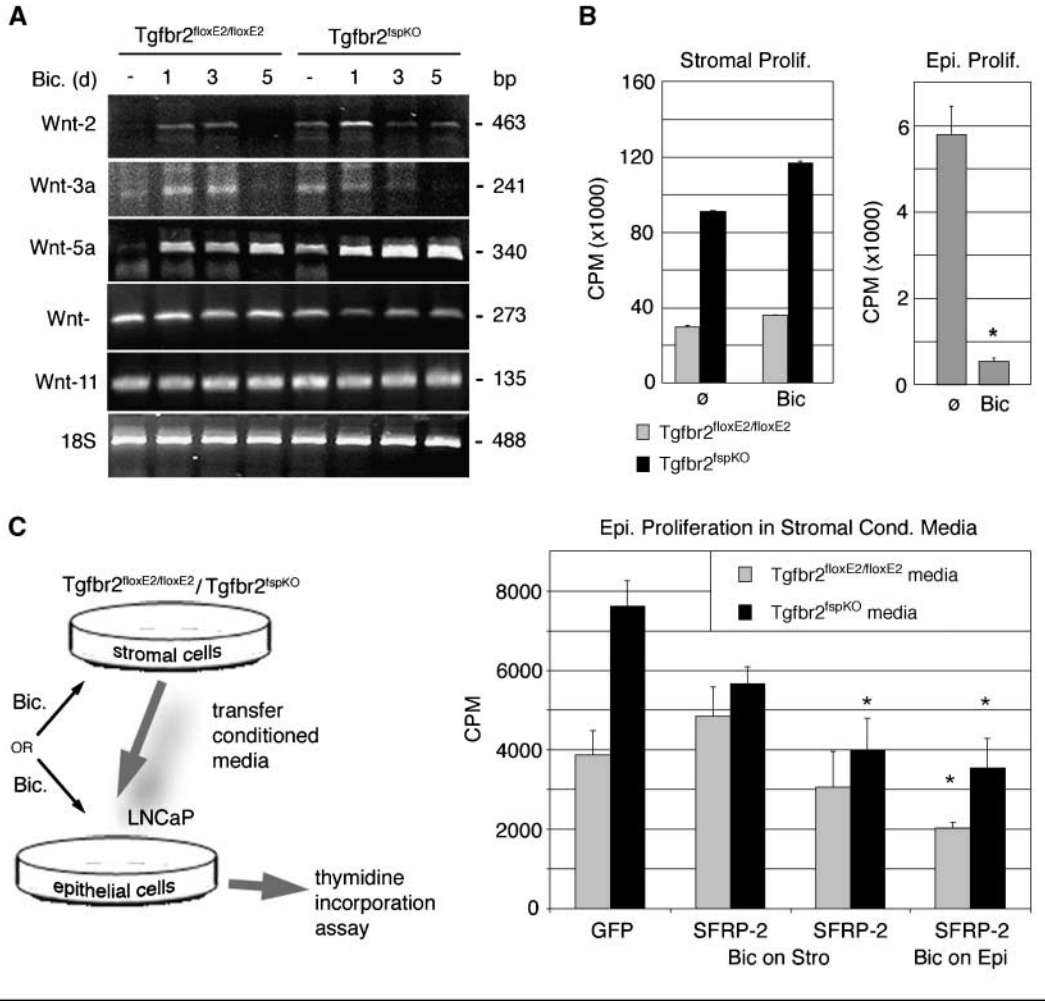

Figure 5. Wnt signaling induced by androgen ablation of stromal cells affects epithelial proliferation. *A,* Tgfbr2$^{floxE2/floxE2}$ and Tgfbr2^{fspKO} stromal cells were treated with bicalutamide over 5 d to analyze Wnt gene expression by semiquantitative RT-PCR. The expression of 18S rRNA was used as a loading control. The results shown are representative of three or more sets of RNA used to test each Wnt gene. *B,* [^{3}H]thymidine incorporation assays were performed on Tgfbr2$^{floxE2/floxE2}$ and Tgfbr2^{fspKO} stromal cells transduced with GFP-adenovirus and grown either in media containing testosterone or bicalutamide (*Bic*) in the absence of testosterone. [^{3}H]Thymidine incorporation assays were performed on LNCaP epithelial cells also treated with or without bicalutamide for 5 d. *Columns,* average of three or more replicates; *bars,* SD. Asterisks indicate significance compared with the respective control. GFP-Tgfbr2$^{floxE2/floxE2}$ stromal cells were not significantly affected by bicalutamide treatment compared with control GFP-Tgfbr2$^{floxE2/floxE2}$ stromal cells ($P = 0.0580$). GFP-Tgfbr2^{fspKO} stromal cells had a significant increase in proliferation with bicalutamide treatment compared with control GFP-Tgfbr2^{fspKO}stromal cells ($P = 0.0016$). LNCaP epithelial cells treated with bicalutamide proliferated significantly slower than untreated LNCaP cells ($P = 0.0025$). Data are representative of three or more individual experiments. *C, left,* a cartoon of the generation of conditioned media is shown. Conditioned media was collected from Tgfbr2$^{floxE2/floxE2}$ or Tgfbr2^{fspKO} stromal cells and used to treat the target LNCaP epithelial cells. *Right,* bar graphs show the results of these conditioned media experiments. Androgen responsive proliferation of LNCaP cells was measured in response to a 120-h treatment with conditioned stromal cell media from Tgfbr2$^{floxE2/floxE2}$ or Tgfbr2^{fspKO} cells by [^{3}H]thymidine incorporation assays. Tgfbr2$^{floxE2/floxE2}$ and Tgfbr2^{fspKO} stromal cells were transduced either with GFP adenovirus as a control or Wnt antagonist SFRP-2 adenovirus before starting collection of conditioned media. *Bic on Stro,* bicalutamide was added to stromal cell cultures during the generation of conditioned media; *Bic on Epi,* bicalutamide was added to epithelial LNCaP cells simultaneously with stromal conditioned media treatment. *Columns,* average of three or more replicates; *bars,* SD. Compared with the GFP control, *P* values for SFRP-2–Tgfbr2$^{floxE2/floxE2}$ conditions are 0.207, 0.339, and 0.011 and for SFRP-2–Tgfbr2^{fspKO} conditions 0.002, 0.005, and 0.004, respectively. Each asterisk indicates statistical significance between the control and knockout data points for a given condition with a *P* value of <0.05 according to a Student's *t* test evaluation.

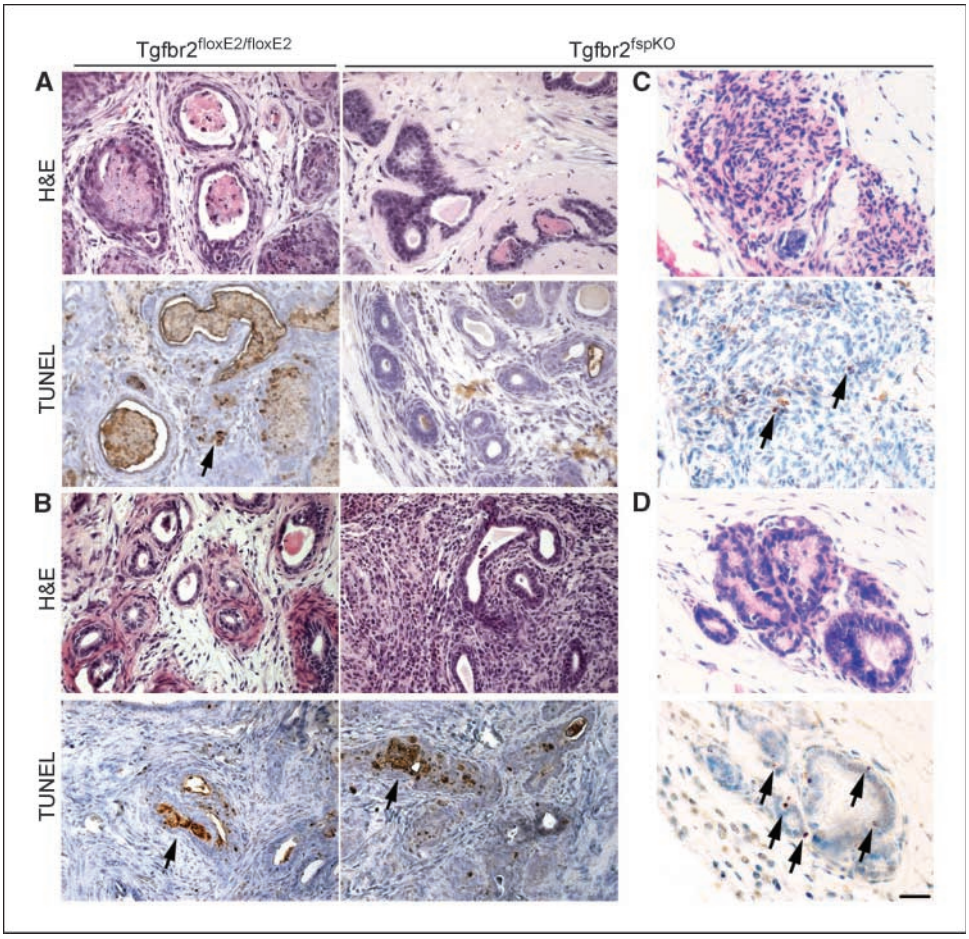

Figure 6. Inhibition of Wnt signaling restores Tgfbr2^{fspKO} prostate responsiveness to androgen ablation. *A,* Tgfbr2$^{floxE2/floxE2}$ or Tgfbr2^{fspKO} mature mouse prostates were transduced with GFP adenovirus and allografted in the renal capsules of male SCID mice. Host mice were castrated for 3 d. Tissues were harvested on day 6 (n = 12) and subjected to H&E staining (*top*), as well as TUNEL staining (*bottom*) for apoptotic cells (*brown*). *B,* Tgfbr2$^{floxE2/floxE2}$ or Tgfbr2^{fspKO} mature mouse prostates were transduced with SFRP-2 adenovirus and allografted in the renal capsules of male SCID mice. Host mice were castrated for 3 d. Tissues were harvested on day 6 (n = 12) and subjected to H&E staining (*top*), as well as TUNEL staining (*bottom*) for apoptotic cells (*brown*). Percentage of positive epithelial TUNEL-positive staining was not statistically different between GFP-Tgfbr2$^{floxE2/floxE2}$ and SFRP-2–Tgfbr2$^{floxE2/floxE2}$ allografts (P = 0.2819). Percentage of positive epithelial TUNEL positive staining in SFRP-2–Tgfbr2^{fspKO} allografts was statistically greater than GFP-Tgfbr2^{fspKO} allografts (P = 0.0373). *C,* tissue recombinations of 12T7f LADY epithelial organoids and Tgfbr2^{fspKO} prostatic stromal cells were allografted in SCID mice for 6 wk. The host mice were given GFP adenovirus throughout the grafting period. Host mice were castrated 7 d before harvesting the prostatic grafts. Tissue recombinants were harvested at week 6 (n = 4) and subjected to H&E staining (*top*), as well as TUNEL staining (*bottom*) for apoptotic cells (*brown*). *D,* tissue recombinations of 12T7f LADY epithelial organoids and Tgfbr2^{fspKO} prostatic stromal cells were allografted in SCID mice for 6 wk. The host mice were given SFRP-2 adenovirus throughout the grafting period. Host mice were castrated 7 d before harvesting the prostatic grafts. Tissue recombinants were harvested at week 6 (n = 4) and subjected to H&E staining (*top*), as well as TUNEL staining (*bottom*) for apoptotic cells (*brown*). Percentage of positive epithelial TUNEL-positive staining in tissue recombinations of 12T7f LADY epithelial organoids and SFRP-2–Tgfbr2^{fspKO} allografts was statistically greater than those in tissue recombinations of 12T7f LADY epithelial organoids and GFP-Tgfbr2^{fspKO} allografts (P = 0.0472). *Scale bar,* 25 μm.

androgens. LNCaP cells, used in our coculture studies, are human prostate cancer lymph node metastatic lesion that lack a functional TGF-β type II receptor and have a functional, yet mutant, androgen receptor (39). The LNCaP cells, analogous to the Tgfbr2$^{NKX3.1KO}$ prostates, enabled us to show that androgen responsiveness mediated by the stroma is not dependent on epithelial TGF-β signaling. Antagonizing Wnt signaling in the absence of androgen ablation in Tgfbr2$^{floxE2/floxE2}$ and Tgfbr2^{fspKO} prostates did not induce apoptosis (Fig. 6). Thus, although TGF-β and androgen signaling converge in the stroma to affect Wnt signaling, they act through distinct pathways.

We showed that activated canonical Wnt signaling helps to limit prostatic regression. It is known that Wnt ligands bind Frizzled receptors on the epithelial surface and transmit signals through the canonical pathway that activates β-catenin/TCF in the nucleus (40). Activating mutations in β-catenin have been identified to affect androgen receptor transcriptional activity and ligand specificity (33, 34). Based on the specific TCF/β-catenin activity in the proximal prostatic ducts of the castrated Tgfbr2$^{floxE2/floxE2}$/TOPGal mice, the mechanism for the survival of the proximal ducts may be through an initial activation of epithelial canonical Wnt signaling. Comparing the Tgfbr2$^{floxE2/floxE2}$/TOPGal and Tgfbr2^{fspKO}/TOPGal mice, it was evident that TGF-β signaling is important to regulate the spatial localization of Wnt signaling to enable regression of the distal ducts in a temporal coordination with androgen signaling. This is consistent with studies showing androgen-induced regeneration occurring at the distal tips of the prostate (41). One mechanism by which the localization of Wnt signaling is limited could be due to secreted Wnt inhibitors (e.g., SFRP-2, DKK-1) in the distal glands. Long-term androgen ablation responses were not studied, as the focus of the study was to determine the role of the

immediate up-regulation of TGF-β after androgen ablation. However, as the prostate continues to regress after day 7, Wnt signaling apparently is replaced by another mechanism to prevent continued regression of the proximal ducts. The latter events and maintenance of the regressed prostate is through a separate mechanism that is more dependent on the availability of androgens because some prostate regression was observed in $Tgfbr2^{fspKO}$ mice 14 days after castration (Fig. 2).

Together, the up-regulation of TGF-β expression in the prostate, coincident with androgen ablation, would support the regression of the prostate by antagonizing stromal Wnt expression brought on from an androgen-regulated mechanism. In normal proximal prostatic tissue, the epithelial Frizzled receptor is activated resulting in canonical, and possibly noncanonical, Wnt signaling, which may contribute to the phenotypes seen in our mouse models. However, based on previous reports that canonical Wnt signaling supports survival and proliferation (21, 42), this is the most likely mechanism that maintains the viability of proximal prostate tissues in the context of androgen ablation. The entire prostate does not involute in the absence of androgens, because subsequent replacement of testosterone results in the regeneration of prostatic tissue (43). Intriguingly, in other mammals, such as deer, antler regeneration is reported to show a site-specific Wnt signaling activation during regeneration (12). The fact that activating mutations of β-catenin are found in androgen-independent prostate cancers (33) suggests that cancer cells can hijack the same Wnt signaling pathways used to support proximal prostate survival to aid in tumor survival. Understanding paracrine interactions of TGF-β, androgen, and Wnt signaling in regulating prostate regression may be linked to its regeneration after androgen supplementation.

Stromal-epithelial interactions have proved to be important in embryonic development and tumorigenesis. Based on the Knudson multihit hypothesis of tumor development, we attempted to further the progression of the PIN lesions associated with LADY 12T7f epithelia, expressing the large T antigen, by recombining them with $Tgfbr2^{fspKO}$ prostatic stromal cells, as the second mutagenic hit (44). Figure 6 illustrated that the Wnt signaling associated with the $Tgfbr2^{fspKO}$ cells not only enabled the PIN lesions to progress to adenocarcinoma, but also enabled the epithelia to become resistant to androgen ablation. Inhibition of Wnt signaling with SFRP-2 seemed to restore androgen sensitivity and decrease tumorigenicity of the resulting tumors. Future prostate cancer therapies would most likely benefit by not only antagonizing the traditional androgen signaling pathway, but also inhibiting Wnt signaling. This would allow therapies to target both the epithelial and stromal compartments, as well as androgen-dependent and androgen-independent tumor cells.

Disclosure of Potential Conflicts of Interest

No potential conflicts of interest were disclosed.

Acknowledgments

Received 11/19/2007; revised 3/19/2008; accepted 4/23/2008.

Grant support: NIH grants CA108646 and CA126505, Department of Defense grants DAMD17-02-1-0063 and W81XWH-04-1-0046, institutional training grants GM062459 and CA09592, and NIH grant FGM079879A (V.R. Placencio). NIH grants CA115985 and DK076602 (M.M. Shen) supported the generation of Nkx3.1 Cre mice.

The costs of publication of this article were defrayed in part by the payment of page charges. This article must therefore be hereby marked *advertisement* in accordance with 18 U.S.C. Section 1734 solely to indicate this fact.

We thank Dr. Elaine Fuchs (Rockefeller Institute) for consent to use the TOPGal mice and Dr. Sanjoy Das (Vanderbilt University) for the SFRP-2 adenovirus.

References

1. Jemal A, Tiwari RC, Murray T, et al. Cancer statistics, 2004. CA Cancer J Clin 2004;54:8–29.
2. Cunha GR, Donjacour AA. Mesenchymal-epithelial interactions in the growth and development of the prostate. Cancer Treat Res 1989;46:159–75.
3. Cunha GR, Chung LW. Stromal-epithelial interactions-I. Induction of prostatic phenotype in urothelium of testicular feminized (Tfm/y) mice. J Steroid Biochem 1981;14:1317–24.
4. Donjacour AA, Cunha GR. Assessment of prostatic protein secretion in tissue recombinants made of urogenital sinus mesenchyme and urothelium from normal or androgen-insensitive mice. Endocrinology 1993;132:2342–50.
5. Kurita T, Wang YZ, Donjacour AA, et al. Paracrine regulation of apoptosis by steroid hormones in the male and female reproductive system. Cell Death Differ 2001; 8:192–200.
6. Cunha GR, Lung B. The possible influence of temporal factors in androgenic responsiveness of urogenital tissue recombinants from wild-type and androgen-insensitive (Tfm) mice. J Exp Zool 1978;205: 181–93.
7. Prins GS, Cooke PS, Birch L, et al. Androgen receptor expression and 5α-reductase activity along the proximal-distal axis of the rat prostatic duct. Endocrinology 1992;130:3066–73.
8. Lee C, Sensibar JA, Dudek SM, Hiipakka RA, Liao ST. Prostatic ductal system in rats: regional variation in morphological and functional activities. Biol Reprod 1990;43:1079–86.
9. Rouleau M, Leger J, Tenniswood M. Ductal heterogeneity of cytokeratins, gene expression, and cell death in the rat ventral prostate. Mol Endocrinol Baltimore 1990; 4:2003–13.
10. Verras M, Sun Z. Roles and regulation of Wnt signaling and β-catenin in prostate cancer. Cancer Lett 2006;237:22–32.
11. Terry S, Yang X, Chen MW, Vacherot F, Buttyan R. Multifaceted interaction between the androgen and Wnt signaling pathways and the implication for prostate cancer. J Cell Biochem 2006;99:402–10.
12. Mount JG, Muzylak M, Allen S, Althnaian T, McGonnell IM, Price JS. Evidence that the canonical Wnt signalling pathway regulates deer antler regeneration. Dev Dyn 2006;235:1390–9.
13. Kyprianou N, Isaacs JT. Expression of transforming growth factor-β in the rat ventral prostate during castration-induced programmed cell death. Mol Endocrinol Baltimore 1989;3:1515–22.
14. Hsing AY, Kadomatsu K, Bonham MJ, Danielpour D. Regulation of apoptosis induced by transforming growth factor-β1 in nontumorigenic rat prostatic epithelial cell lines. Cancer Res 1996;56:5146–9.
15. Brodin G, ten Dijke P, Funa K, Heldin CH, Landstrom M. Increased smad expression and activation are associated with apoptosis in normal and malignant prostate after castration. Cancer Res 1999;59:2731–8.
16. Massague J, Gomis RR. The logic of TGFβ signaling. FEBS Lett 2006;580:2811–20.
17. Hayes SA, Zarnegar M, Sharma M, et al. SMAD3 represses androgen receptor-mediated transcription. Cancer Res 2001;61:2112–8.
18. Chipuk JE, Cornelius SC, Pultz NJ, et al. The androgen receptor represses transforming growth factor-β signaling through interaction with Smad3. J Biol Chem 2002; 277:1240–8.
19. Kang HY, Lin HK, Hu YC, Yeh S, Huang KE, Chang C. From transforming growth factor-β signaling to androgen action: identification of Smad3 as an androgen receptor coregulator in prostate cancer cells. Proc Natl Acad Sci U S A 2001;98:3018–23.
20. Yang X, Chen MW, Terry S, et al. Complex regulation of human androgen receptor expression by Wnt signaling in prostate cancer cells. Oncogene 2006;25:4256.
21. Widelitz R. Wnt signaling through canonical and non-canonical pathways: recent progress. Growth Factors 2005;23:111–6.
22. Bhowmick NA, Chytil A, Plieth D, et al. TGF-β signaling in fibroblasts modulates the oncogenic potential of adjacent epithelia. Sci New York NY 2004;303:848–51.
23. Chytil A, Magnuson MA, Wright CV, Moses HL. Conditional inactivation of the TGF-β type II receptor using Cre:Lox. Genesis 2002;32:73–5.
24. DasGupta R, Fuchs E. Multiple roles for activated LEF/TCF transcription complexes during hair follicle development and differentiation. Development (Cambridge, England) 1999;126:4557–68.
25. Kasper S, Sheppard PC, Yan Y, et al. Development, progression, and androgen-dependence of prostate tumors in probasin-large T antigen transgenic mice: a model for prostate cancer. Lab Investig A J Technical Methods Pathol 1998;78:i–xv.
26. Shappell SB, Thomas GV, Roberts RL, et al. Prostate pathology of genetically engineered mice: definitions and classification. The consensus report from the Bar Harbor meeting of the Mouse Models of Human Cancer Consortium Prostate Pathology Committee. Cancer Res 2004;64:2270–305.
27. Tuxhorn JA, Ayala GE, Smith MJ, Smith VC, Dang TD, Rowley DR. Reactive stroma in human prostate cancer: induction of myofibroblast phenotype and extracellular matrix remodeling. Clin Cancer Res 2002;8:2912–23.

28. Roberts AB, Sporn MB, Assoian RK, et al. Transforming growth factor type β: rapid induction of fibrosis and angiogenesis *in vivo* and stimulation of collagen formation *in vitro*. Proc Natl Acad Sci U S A 1986;83:4167–71.
29. Bhowmick NA, Ghiassi M, Bakin A, et al. Transforming growth factor-β1 mediates epithelial to mesenchymal transdifferentiation through a RhoA-dependent mechanism. Mol Biol Cell 2001;12:27–36.
30. Hayward SW, Haughney PC, Rosen MA, et al. Interactions between adult human prostatic epithelium and rat urogenital sinus mesenchyme in a tissue recombination model. Differentiation 1998;63:131–40.
31. Strutz F, Okada H, Lo CW, et al. Identification and characterization of a fibroblast marker: FSP1. J Cell Biol 1995;130:393–405.
32. Hayward SW. Approaches to modeling stromal-epithelial interactions. J Urol 2002;168:1165–72.
33. Voeller HJ, Truica CI, Gelmann EP. β-Catenin mutations in human prostate cancer. Cancer Res 1998; 58:2520–3.
34. Truica CI, Byers S, Gelmann EP. β-Catenin affects androgen receptor transcriptional activity and ligand specificity. Cancer Res 2000;60:4709–13.
35. Chen G, Shukeir N, Potti A, et al. Up-regulation of Wnt-1 and β-catenin production in patients with advanced metastatic prostate carcinoma: potential pathogenetic and prognostic implications. Cancer 2004;101:1345–56.
36. Galli LM, Barnes T, Cheng T, et al. Differential inhibition of Wnt-3a by Sfrp-1, Sfrp-2, and Sfrp-3. Dev Dyn 2006;235:spc1.
37. Hou X, Tan Y, Li M, Dey SK, Das SK. Canonical Wnt signaling is critical to estrogen-mediated uterine growth. Mol Endocrinol 2004;18:3035–49.
38. Liu XH, Kirschenbaum A, Yao S, Liu G, Aaronson SA, Levine AC. Androgen-induced Wnt signaling in preosteoblasts promotes the growth of MDA-PCa-2b human prostate cancer cells. Cancer Res 2007;67: 5747–53.
39. Kim IY, Zelner DJ, Sensibar JA, et al. Modulation of sensitivity to transforming growth factor-β 1 (TGF-β 1) and the level of type II TGF-β receptor in LNCaP cells by dihydrotestosterone. Exp Cell Res 1996;222:103–10.
40. Yardy GW, Brewster SF. Wnt signalling and prostate cancer. Prostate Cancer Prostatic Dis 2005;8:119–26.
41. Sugimura Y, Cunha GR, Donjacour AA, Bigsby RM, Brody JR. Whole-mount autoradiography study of DNA synthetic activity during postnatal development and androgen-induced regeneration in the mouse prostate. Biol Reprod 1986;34:985–95.
42. Polakis P. Wnt signaling and cancer. Genes Dev 2000; 14:1837–51.
43. Wright AS, Douglas RC, Thomas LN, Lazier CB, Rittmaster RS. Androgen-induced regrowth in the castrated rat ventral prostate: role of 5α-reductase. Endocrinology 1999;140:4509–15.
44. Knudson AG, Jr., Hethcote HW, Brown BW. Mutation and childhood cancer: a probabilistic model for the incidence of retinoblastoma. Proc Natl Acad Sci U S A 1975;72:5116–20.